Mixtures of octanol and an ionic liquid: structure and transport

Man Zhao,^{1, a)} Boning Wu,^{1, b)} and Edward W. Castner Jr.^{1, c)}

Department of Chemistry and Chemical Biology, Rutgers,

The State University of New Jersey, Piscataway, NJ 08854

Ionic liquids (ILs) with long alkyl substituents are amphiphilic, which leads to a bicontinuous liquid structure. The strongly interacting anionic and cationic head groups form a long range charge network, with the hydrocarbon tails forming a nonpolar domain. Such nonpolar domains have been shown to dissolve a variety of neutral organic solvents. In mixtures of ionic liquids with neutral solvents, the organic molecules residing in the nonpolar domains experience different environment and friction from the charged cations and anions, and thus diffuse much faster than predicted by hydrodynamic scaling using the average viscosity of the mixture. In this work, we report studies of the structure and transport properties for mixtures of 1-octanol with the IL trihexyltetradecylphosphonium bis(trifluoromethylsulfonyl)imide $(P_{6,6,6,14}^+/NTf_2^-)$. The majority of the atom fraction in the $P_{6,6,6,14}^{+}$ cation comprises the four hydrocarbon substituents. The unique amphiphilic nature of ILs with the $P_{6,6,6,14}$ cation makes 1-octanol fully miscible with the IL at ambient temperatures. X-ray scattering experiments show that the ionic liquid structure persists in the mixtures for 1-octanol mole fractions as large as $x_{oct} = 0.90$. The self-diffusion coefficients of the three molecular species in the mixtures were measured by NMR experiments. The self-diffusion of the $P_{6,6,6,14}$ cation is well described by the Stokes-Einstein equation, while the diffusivity of NTf₂⁻ anion is slightly lower than the hydrodynamic prediction. The measured diffusivities of octanol in these mixtures are 1.3-4 times higher than the hydrodynamic predictions.

Keywords: ionic liquid, mixtures, X-ray scattering, transport

^{a)} Haisco Pharmaceutical Group, No. 136 Baili Road, Wenjiang District, Chengdu, Sichuan Province, China.

b) Present address: Department of Chemistry, Stanford University, Palo Alto, CA 94305

c) ecastner@chem.rutgers.edu

INTRODUCTION

Ionic liquids (ILs) are molten salts that remain liquid near ambient temperatures. The unique properties of the molecular anions and cations lead to a range of unique physical and chemical properties.^{1–4} These properties have led to a wide range of applications for ILs in separations, energy storage devices, and a variety of other applications in the energy and environmental fields.^{5–10} Since chemical separations are energy intensive, ILs have been widely investigated as a means to more efficient separations of gases and liquids, especially hydrocarbons and fluorocarbons.^{11–15}

The strong electrostatic interactions between anions and cations lead to ordered liquid structures both for molten salts and for ionic liquids with larger molecular ions. These charge-ordered liquid structures become bicontinuous when either the anions or cations are amphiphilic. When the cations or anions have sufficiently long alkyl tails, these tails form nonpolar nanoscale domains.^{2,16–24} A signature for the existence of nanoscale domains is the observation of a first sharp diffraction peak (FSDP) in the total liquid structure function S(q), which is obtained from X-ray and neutron scattering experiments and from molecular simulations.^{16,18–20,25} The heterogeneity of IL structures is also connected to the dynamic complexity in ILs.²⁶

Though the viscosities, diffusivities and conductivities of ILs can be easily measured, these reflect the averaged properties. The amphiphilic nature of many ILs can lead to increased structural and dynamical heterogeneity when a neutral molecular species is mixed with the IL.^{27–29} Water and organic solvents are the most common solutes to be mixed with ILs.^{30–35}

Blesic, et al. studied the solubility of alkanes, alkanols and their fluorinated counterparts in ILs with tetraalkylphosphonium and other alkylated cations.³¹ The trihexyltetrade-cylphosphonium ($P_{6,6,6,14}^+$) based ILs show very high solubilities of neutral organic species. This is especially true for the $P_{6,6,6,14}^+$ /NTf₂⁻ IL, which is totally miscible with several alkanols including 1-octanol.³¹ Blesic, et al. showed that up to 2/3 volume fraction of hydrocarbons (90% mole fraction for hexane) can be dissolved in $P_{6,6,6,14}^+$ /NTf₂⁻.³¹ They also demonstrated that the solubility of alkanes was much lower in an imidazolium based IL with a single tetradecyl chain, 1-methyl-3-tetradecylimidazolium bis(trifluoromethylsulfonyl)imide (C[14]mim⁺/NTf₂⁻) than in $P_{6,6,6,14}^+$ /NTf₂⁻.³¹

The remarkable results of Blesic, et al.³¹ inspired us to study the structural and dynamical

properties of both alcohols and alkanes in $P_{6,6,6,14}^+/NTf_2^-$. The structural properties of ILs with other tetraalkylphosphonium cations have been studied by X-ray scattering and NMR.^{20,36} ILs with the $P_{6,6,6,14}^+$ cation have been well characterized using X-ray scattering for the cases of both the chloride and NTf_2^- anions.^{37–40}

In this work, we report the structural properties of mixtures containing 1-octanol and $P_{6,6,6,14}^+/NTf_2^-$, obtained from high photon-energy X-ray scattering data.⁴¹ The self-diffusion coefficients of the NTf_2^- anion, the $P_{6,6,6,14}^+$ cation, and 1-octanol are measured using the pulse-gradient spin echo (PG-SE) NMR method, ^{42–44} using the ¹⁹F signal for NTf_2^- and ¹H signals for $P_{6,6,6,14}^+$ and 1-octanol. The molecular transport data are compared with the bulk transport properties that are obtained from viscosity measurements.

Our previous study of mixtures of hexane (C_6D_{14}) with the $P_{6,6,6,14}^+/NTf_2^-$ IL revealed that the characteristic structure of the IL^{37–40} remained present even up to 80% mole fraction of hexane at room temperature.²⁷ The explanation for this unexpected behavior is that the non-polar domains created by nanophase segregation between the anionic and cationic polar head groups and the cationic hydrocarbon tails lead to a hydrocarbon-rich domain that is capable of solubilizing the hexane. NMR self-diffusion measurements revealed that the non-polar hydrocarbon domain has a very different local friction than the domain comprising the polar head groups.²⁷ In the $P_{6,6,6,14}^+/NTf_2^-$ solutions with hexane, the neutral hydrocarbon was found to have a self-diffusivity that was on average 21 times larger than the $P_{6,6,6,14}^+$ cation.²⁷ The size differences between the $P_{6,6,6,14}^+$ and the hexane would lead to a ratio of 1:1.8 in the diffusivities based on predictions from the Stokes-Einstein hydrodynamic law, so these predictions were off by more than an order of magnitude compared to the measured diffusivities.²⁷

A common element between our previous study of the structure and dynamics of the $P_{6,6,6,14}^+/NTf_2^-$ -hexane mixtures and the present study of octanol in the same IL is that the intrinsic liquid structure of the IL persists across the range of concentrations measured. However, there is also a subtle difference between our two studies, which is that unlike hexane, 1-octanol has an intrinsic liquid structure that results from a network of molecular chains formed by H-bond donation by the hydroxyl proton and H-bond accepting by the hydroxyl oxygen. Such a networked structure is the reason why 1-octanol and other alcohols exhibit a first sharp diffraction peak in the liquid structure function. $^{18-20,45}$ In the $P_{6,6,6,14}^+/NTf_2^-$ -octanol mixtures, the octyl chain resides in the nonpolar domain, and H-

bonding at the terminal hydroxyl group can lead to strong interactions with polar regions of the liquid.^{46–48} In this mixture the stronger ionic interactions dominate the structure formation, although for very high fractions of octanol, undoubtedly both H-bonded and ionic network morphologies contribute to the structure observed in the X-ray scattering pattern.

EXPERIMENTAL METHODS

Sample Preparation

The $P_{6,6,6,14}^+/NTf_2^-$ ionic liquid was purchased from IoLiTec in ultra-high purity grade and dried under vacuum with stirring for 48 h before use. Neat anhydrous 1-octanol was purchased from Sigma-Aldrich and used as received. The mixtures of $P_{6,6,6,14}^+/NTf_2^-$ and 1-octanol were prepared in a glove box under an argon atmosphere, where the oxygen and water concentrations were below 0.1 ppm and 0.4 ppm, respectively. In addition to the neat $P_{6,6,6,14}^+/NTf_2^-$ and 1-octanol samples, eight $P_{6,6,6,14}^+/NTf_2^-$ -octanol mixtures were prepared for X-ray structural studies with 1-octanol mole fractions of $x_{oct} = 0.1$, 0.3, 0.5, 0.65, 0.8, 0.9, 0.95 and 0.98. Each sample was put in 2 mm o.d. quartz capillaries (Hampton Research) and temporarily sealed with beeswax in the glove box. After removal from the glovebox, the capillaries were immediately flame sealed with a natural gas-oxygen torch.

High-energy X-ray Scattering Experiments

The capillaries prepared as described above were used for high photon-energy synchrotron-based X-ray scattering experiments. The experiments were performed at the Advanced Photon Source (APS) beamline 11-ID-B for pair distribution function analysis. The X-ray beam wavelength was 0.2114 Å, corresponding to a photon energy of 58.66 keV. Use of such high X-ray photon energies minimizes the possibility of radiation damage to the samples. The sample-to-detector distance was calibrated using a powdered CeO₂ test sample and calculated to be 22.7 cm, resulting in scattering data in the range between $0.2 \le q \le 20$ Å⁻¹. The Fit2D⁴⁹ program was used to correct and integrate the raw X-ray intensities and the PDFgetX2 program⁵⁰ was used to transform the corrected data into the total structure factors S(q). The experimental protocols and data analysis procedures have been described previously in detail. $^{20,22-24,27,51-55}$

Viscosity Measurements

A Cambridge Viscosity Viscolab 4100 viscometer was used to measure the temperature-dependent viscosities of the $P_{6,6,6,14}^+/NTf_2^-$ -octanol mixtures. The procedures were described in detail previously.⁵⁶ The temperature set point for the measurements was regulated to ± 0.1 K using a Lauda RM-6 recirculating water bath. Viscosities were recorded at 20, 25, 30, 35, and 40 °C.

Diffusivity Measurements by PG-SE NMR

The PG-SE NMR technique^{42–44} was used to measure the self-diffusion coefficients in the IL, 1-octanol and mixture samples. The sealed capillaries prepared as described above were placed inside standard 5 mm outer diameter NMR tubes that contained 99.9% D_2O to provide a deuterium lock signal. A Varian Direct Drive NMR instrument at a 400 MHz 1H frequency was used to measure the PG-SE intensities as a function of applied gradient magnetic field strength g, using procedures described previously. 27,52,55,57,58 The specific diffusion-ordered spectroscopy (DOSY) pulse sequence used was the Bipolar Pulse Pair Stimulated Echo sequence (called DBPPSTE in the Varian DirectDrive software). 44 The gradient field strength g was varied between 5 to 350 G/cm. The self-diffusion coefficient D is obtained by fitting the spin echo intensities to the following equation:

$$I(g) = I(0) \exp\left(-D(\gamma g \delta)^2 (\Delta - \delta/3)\right) \tag{1}$$

where I(g) is the intensity of the signal, I(0) is the intensity of the signal at g = 0, γ is the gyromagnetic ratio, δ is the duration of the gradient pulse, Δ is diffusion delay, and D is the diffusion coefficient.⁴³

Self-diffusion coefficients for the cation $P_{6,6,6,14}^+$ and 1-octanol were measured using 1H signals, while those for the NTf_2^- anion were measured using the single ^{19}F peak. The measurements were carried out at three temperatures: 298, 308 and 318 K. Samples were re-equilibrated for at least 10 min after each temperature change.

RESULTS AND DISCUSSION

Structure functions S(q) of the IL-octanol mixtures

Fig. 1 presents the liquid structure functions S(q) measured using high-energy X-ray experiments for neat $P_{6,6,6,14}^+/NTf_2^-$, neat 1-octanol and their mixtures. For each S(q), there is a clear separation between intermolecular and intramolecular correlations at q = $2.0~{\rm \AA^{-1}}$ as has been observed for neat ${\rm P_{6,6,6,14}}^+/{\rm Cl^{-37}}$ and for neat ${\rm P_{6,6,6,14}}^+/{\rm NTf_2^-}.^{38-40}$ Three intermolecular peaks are observed for the neat $P_{6,6,6,14}^+/NTf_2^-$ IL: the adjacency peak at $q = 1.37 \text{ Å}^{-1}$ resulting from near-neighbor interactions; the charge-charge correlation peak at $q = 0.75 \text{ Å}^{-1}$ that arises from the second-shell structure of like-charge ions, and the FSDP at $q = 0.41 \text{ Å}^{-1}$, indicating the intermediate range order that results from the hydrophobic domains created by interactions of the hydrocarbon tails on the $P_{6.6,6.14}$ ⁺ cation. ^16,20,38–40,51 We note that although the charge-charge correlation peak at $q=0.75~{\rm \AA}^{-1}$ appears only as a shoulder in the full X-ray S(q) data, the same peak analyzed using the ionic partitioning of S(q) obtained from MD simulations reveals the strongest correlation, with greater amplitude than either the adjacency peak or FSDP.³⁸ The small amplitude observed for the charge-charge correlation peak has previously been shown to result from the nearly complete destructive interference between the anion-anion and cation-cation peaks and the anion-cation peaks. 24,38,51,59,60

The adjacency peak in S(q) at $q = 1.37 \text{ Å}^{-1}$ shows only negligible changes in amplitude across the range of concentrations shown in the inset of Fig. 1. We note that the adjacency peak for neat 1-octanol is observed at $q = 1.40 \text{ Å}^{-1}$, thus fully overlapping with that for the IL. As the 1-octanol concentration increases, the contribution to the peak at $q = 0.75 \text{ Å}^{-1}$ from the anion-anion and cation-cation interactions of the IL is diminished as a result of the larger amplitude of the lower-q tail of 1-octanol adjacency peak. For $x_{oct} > 0.8$, the $P_{6,6,6,14}^+/\text{NTf}_2^-$ charge correlation peak is no longer observable in the total S(q).

The intensity of the FSDP in S(q) is significantly decreased as the concentration of 1-octanol increases from $x_{oct} = 0$ to 1. The inset shows the S(q) emphasizing the intermolecular interactions for $q < 2 \text{ Å}^{-1}$. The dashed line in the inset indicates the shift in q for the FSDP. The FSDPs for neat 1-octanol and $P_{6,6,6,14}^+/\text{NTf}_2^-$ occur at nearly the same value of $q = 0.41 \text{ Å}^{-1}.61,62$ Therefore, the FSDP first shifts to lower q values as the hydrophobic domains

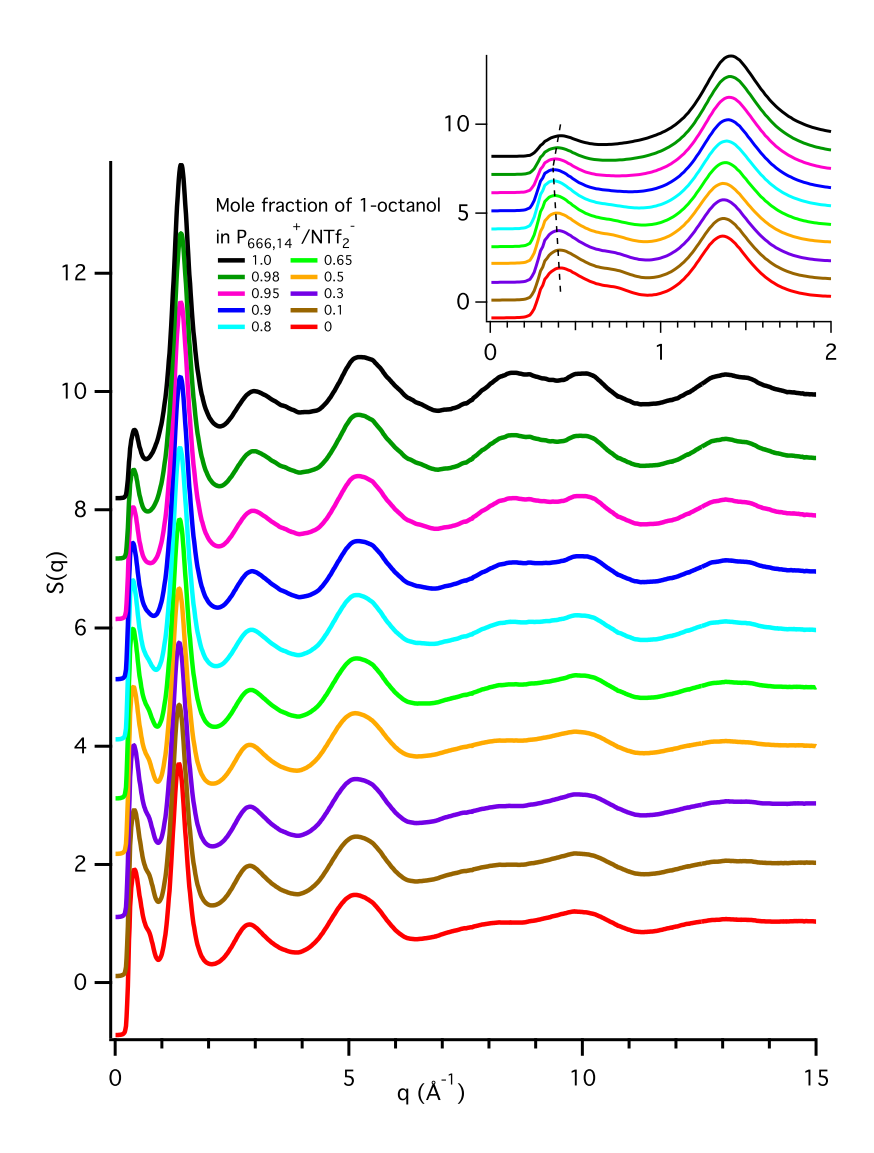


FIG. 1. Liquid structure functions for mixtures of 1-octanol in $P_{6,6,6,14}^+/NTf_2^-$; mole fractions range from $x_{oct} = 0.0$ to 1.0. The inset shows the intra-molecular interactions under 2 Å⁻¹. For clarity, each S(q) is incremented by +1 vertically.

in the $P_{6,6,6,14}^+/NTf_2^-$ IL are swollen by the addition of the octanol. As the fraction of octanol molecules begins to dominate S(q) for $x_{oct} > 0.9$, the FSDP shifts back toward $q = 0.41 \text{ Å}^{-1}$, the value observed for neat 1-octanol. Interpreting the position of the FSDP (q) as a Bragg peak corresponds to a real space domain size of $(2\pi/q)$. The domain grows from an effective size of 15.4 Å for the neat IL to 17.0 Å for the mixtures with $x_{oct} = 0.8$, then shrinks back to 15.4 Å for neat 1-octanol, which indicates that the domain size of the H-bonded network of the pure alcohol coincides with the size of the IL domains at

room temperature. For lower mole fractions of 1-octanol, the alcohol molecules reside in these nonpolar domains formed by the $P_{6,6,6,14}^+$ cations. The addition of octanol expands the nonpolar domains formed by the $P_{6,6,6,14}^+$ cation, so the FSDP shifts to lower q value. As the mole fraction of 1-octanol increases, the system transitions from the case where the 1-octanol molecules are solvated by the IL anions and cations to the case where discrete $P_{6,6,6,14}^+$ and NTf_2^- ions or ion pairs are solvated by 1-octanol molecules. The nonpolar domains in this case are mainly formed by the octyl tails on the 1-octanol. Therefore, the size of the nanoscale domains starts to decreases as the mole fraction of 1-octanol reaches $x_{oct} = 0.8$ or higher. Eventually, the FSDP shifts back to 0.41 Å⁻¹ for neat 1-octanol. Such effects have been discussed in terms of templating effects of the IL charge network by Elfgen, $et\ al.^{64}$

Viscosities of IL-octanol mixtures

Temperature-dependent viscosities were measured for 1-octanol, $P_{6,6,6,14}^+/NTf_2^-$ and their mixtures. The temperature-dependent viscosities are plotted in Fig. 2, with the raw viscosity data and fits of these data to the Arrhenius equation provided in the Supplementary Material. The viscosity of $P_{6,6,6,14}^+/NTf_2^-$ is about 45 times larger than the viscosity of 1-octanol at room temperature, so the addition of 1-octanol to the $P_{6,6,6,14}^+/NTf_2^-$ IL decreases the viscosity of the mixture significantly relative to the neat IL. The temperature dependent viscosities are fit to the VFT equation: $\ln(\eta(T)) = \ln(\eta_{VFT}) + B/(T - T_0)$ with the fits shown as solid lines in Fig. 2.^{56,65} Since the Arrhenius viscosity law is the high temperature limit of the VFT equation, the Arrhenius viscosity activation energies E_{η} can be calculated from the VFT parameters using Eqn. 2 below. The VFT fit parameters and E_{η} values are listed in Table I. The calculated values of effective activation energies E_{η} decrease roughly parabolically with the 1-octanol mole fraction x_{oct} . This result indicates that the ion-ion and alcohol-ion interactions are stronger than the alcohol-alcohol interactions.

$$E_{\eta} \equiv R \frac{d \ln(\eta)}{d(1/T)} = RB \left(\frac{T}{T - T_0}\right)^2 \tag{2}$$

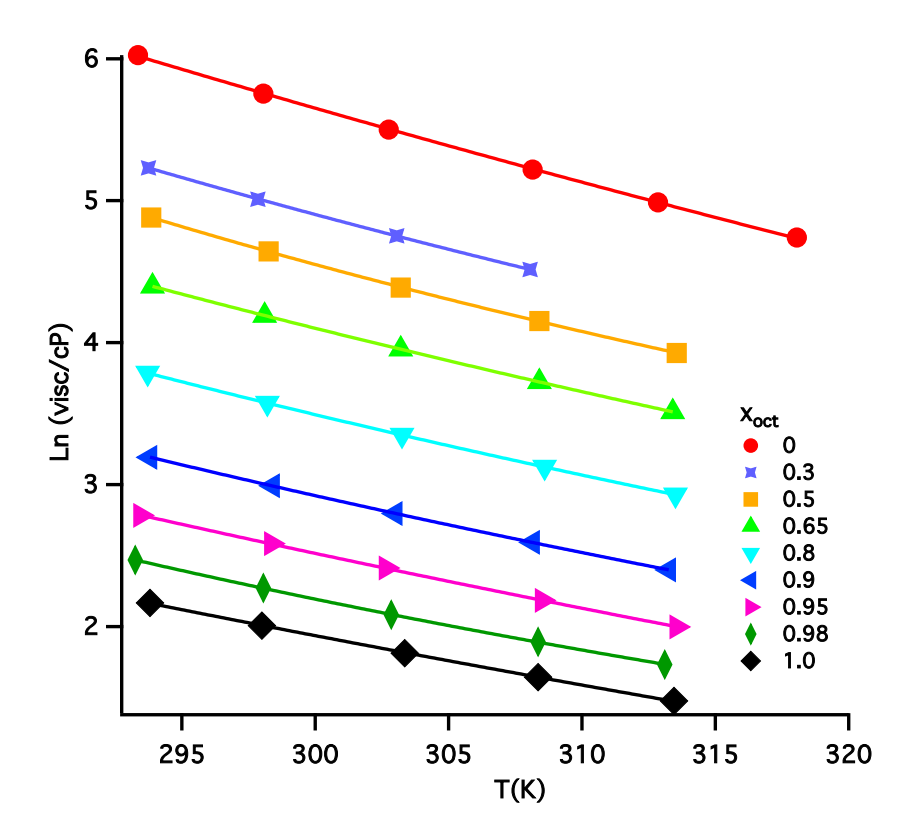


FIG. 2. The temperature-dependent viscosity data fit to the VFT equation for 1-octanol, $P_{6,6,6,14}^+/NTf_2^-$ and their mixtures.

\mathbf{x}_{oct}	η_{VFT}	B	T_0 (K)	$E_{\eta} (kJ/mol)$
0	-5.17	2135.2	102.64	41.3
0.3	-3.30	1334.3	137.46	38.2
0.5	-1.46	706.4	182.52	39.1
0.65	-5.18	1837.1	102.11	35.3
0.8	-4.41	1388.8	124.29	34.0
0.9	-4.89	1443.3	115.23	31.9
0.95	-7.64	2565.8	47.28	30.1
0.98	-2.69	615.5	173.88	29.5
_1	-4.77	1233.5	116.02	27.5

TABLE I. VFT fit parameters for the temperature-dependent viscosities of $P_{6,6,6,14}^+/NTf_2^-$, 1-octanol and the mixtures. x_{oct} is the mole fraction of 1-octanol. E_{η} is calculated using Eq. 2.

Diffusivities of IL-octanol mixtures

The diffusivities for the NTf₂⁻ anion, the P_{6,6,6,14}⁺ cation, and 1-octanol were measured by PG-SE NMR.⁴²⁻⁴⁴ For the NTf₂⁻ anion, diffusivities were measured using the single ¹⁹F NMR line at $\delta = -80$ ppm. The P_{6,6,6,14}⁺ cation diffusivities were measured from the α -carbon methylene group triplets at $\delta = 2.31$ ppm. The 1-octanol diffusivities were measured using the α -carbon methylene peak at $\delta = 3.74$ ppm. Previous error estimates for the PG-SE data remain the same with $\Delta T = \pm 1$ K and a standard deviation for the values of D being 3.5%.⁵² The self-diffusion coefficients were measured for a set of three temperatures: 298, 308, and 318 K. In Fig. 3, all of the self-diffusivities are combined in three master plots of D vs. the ratio of absolute temperature to shear viscosity, T/η , for the NTf₂⁻ anion (top), P_{6,6,6,14}⁺ cation (middle) and 1-octanol (bottom) on log-log axes. This type of plot facilitates discussion of the non-hydrodynamic behavior displayed by these diffusivities. Values of the viscosity for a given temperature are extrapolated from the experimental data using the VFT fit parameters in Table I. The raw diffusivity data are available in the Supplementary Material.

For the neat $P_{6,6,6,14}^+/NTf_2^-$ IL, the anionic and cationic diffusivities qualitatively follow the scaling predicted by the Stokes-Einstein hydrodynamic law $(D \propto T/\eta)$. However, Harris showed that a fractional Stokes-Einstein (FSE) equation, $D \propto (T/\eta)^{\alpha}$, is required to obtain the most accurate fits.⁶⁷ For most ILs, the typical value of α lies in the range $0.9 \le \alpha \le$ $0.95.^{67}$ Using the method of volume increments and assuming spherical molecular shapes,⁶⁸ the effective van der Waals radii r are then calculated to be 3.36, 5.18 and 3.33 Å for NTf_2^- , $P_{6,6,6,14}^+$, and 1-octanol, respectively. To compare our experimental results from PG-SE NMR measurements with predictions of the FSE model, a dashed line is added to the graphs in Fig. 3 using $\alpha = 0.9$ with the slip boundary condition and these effective spherical radii.⁵⁷

The self-diffusivities for the NTf_2^- anion fit well with the FSE model predictions at low 1-octanol mole fractions. When x_{oct} is larger than 0.65, the NTf_2^- anion shows a diffusivity lower than predicted by the S-E theory. For higher octanol mole fractions, the average number of hydrogen bonds with 1-octanol OH groups on each NTf_2^- anion increases with the 1-octanol concentration, which results in the lower diffusivity for the NTf_2^- anion.

The self-diffusivity of the $P_{6.6,6,14}^+$ cation is reasonably well described by slip hydrody-

namics (middle graph). This indicates that the average friction in the mixture, as characterized by the shear viscosity, is strongly correlated with the structural fluctuations of the charge network, which must scale with the self-diffusivities of the $P_{6,6,6,14}^+$ cation and NTf_2^- anion. These concepts have been discussed in detail by Araque, et al.²⁸

In contrast, the self-diffusion behavior of 1-octanol deviates greatly from the SE hydrodynamic predictions, especially at lower mole fractions of octanol in the mixture. For octanol mole fractions in the range of $0.9 < x_{oct} < 1$, the diffusivity of 1-octanol approaches the predictive line from the FSE model. This is likely due to the formation of nanoscale domains in the IL system by the interactions of the alcohol octyl tails with the alkyl tails on the $P_{6,6,6,14}^+$ cations. For smaller values of x_{oct} , the 1-octanol molecules will be solvated in the nonpolar domains formed by the $P_{6,6,6,14}^+$ cations, where they experience a reduced friction for transport through the liquid mixture. The lower friction experienced by the octyl tail is modulated by the strong H-bonding interaction between the octanol hydroxyl group and the NTf₂⁻ oxygen atoms. This is consistent with studies of 1-propanol and 1-butanol in an imidazolium-cation IL with the NTf₂⁻ anion that were reported by Agrawal, et al.⁶⁹ Overall, the octanol in the mixtures with the IL will diffuse faster than predicted by the FSE model. For $n-C_6D_{14}$ in $P_{6,6,6,14}^+/NTf_2^-$, the diffusivity of $n-C_6D_{14}$ is consistently more than an order of magnitude larger than predicted. The self-diffusion of 1-octanol to the S-E prediction ratio is in the range of 1.3 to 4, which is much lower than the ratio range from 16 to 28 for $n-C_6D_{14}$ in $P_{6,6,6,14}^+/NTf_2^-$. For higher octanol concentrations, the IL anions and cations are fully solvated by octanol molecules. Therefore, the solvation environment of 1-octanol molecules in these mixtures is similar to that for the neat alcohol, and the diffusivities for 1-octanol molecules in the mixture approach the predicted values from the scaled hydrodynamic (FSE) model. Such solvation environments for alcohol-IL mixtures have been previously discussed by Murphy, et al. and by Hadrian, et al. and Vaz, et al. 45,47,48 Iwahashi, et al. have proposed that alcohols in ILs form a liquid-liquid interface that can be exploited for a unique solvation environment that has characteristics different from both the alcohol and IL. 70,71

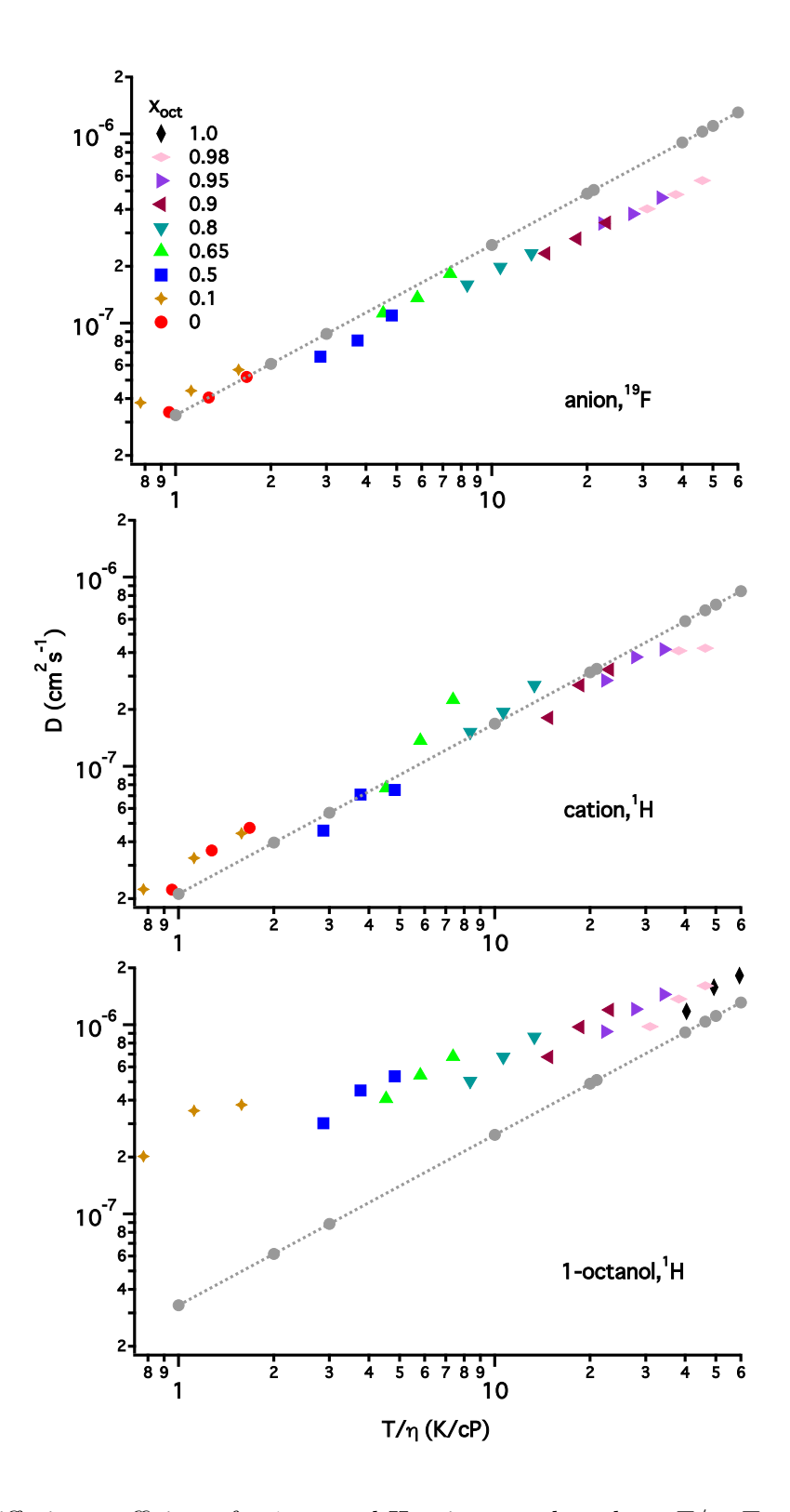


FIG. 3. Self-diffusion coefficients for 1-octanol-IL mixtures plotted vs. T/η . Top: NTf₂⁻; middle: $P_{6,6,6,14}^+$; bottom: 1-octanol. Dashed lines denote the predictions from the fraction Stokes-Einstein equation with $\alpha = 0.9$.

CONCLUSIONS

Addition of 1-octanol to the $P_{6,6,6,14}^+/NTf_2^-$ IL leads to changes of several physical properties.³¹ The characteristic structure of the ionic liquid is retained even for very high concentrations of 1-octanol. The FSDP in the liquid structure functions S(q) shifts to lower q values as the mole fraction of 1-octanol increases. This is consistent with the increase of the average domain size from 15.4 to 17.0 Å. Adding a low viscosity solvent to the viscous IL greatly decreases the viscosity of the solution, which in turn increases the diffusivities of the molecules and ions. The viscosities are well fit by both the Arrhenius and VFT equations in the measured temperature range. The Arrhenius activation energies calculated from the viscosity data show that while the 1-octanol averaged friction is much higher than for an alkane,²⁷ it is still less than the friction deriving from the charged network of the IL.

In the mixtures of 1-octanol and the $P_{6,6,6,14}^+/NTf_2^-$ IL, the self-diffusion coefficients of the $P_{6,6,6,14}^+$ cations and NTf_2^- anions are in moderately good agreement with hydrodynamic predictions, whereas the diffusivities of 1-octanol molecules are significantly faster than predicted. This faster diffusion of 1-octanol in the mixtures is a result of the accommodation of 1-octanol in apolar domains formed by the alkyl tails on the $P_{6,6,6,14}^+$ cations. However, the diffusivity of 1-octanol in $P_{6,6,6,14}^+/NTf_2^-$ is significantly slower relative to our prior results for hexane in the same IL, 27 due to the hydrogen bonding between the hydroxyl group on the 1-octanol and the ions. In conclusion, we suggest that exploitation of the unique structural and transport properties of these mixtures may lead to new opportunities for designer solvents for enhanced chemical reactivity and interface science.

SUPPLEMENTARY MATERIAL

This document provides the raw viscosity and diffusivity data, together with results from fits to the Arrhenius equation.

ACKNOWLEDGMENTS

We gratefully acknowledge support for this work from the National Science Foundation. The work was begun with support from grant CHE-1664809 and completed with support from grant CHE-1954373. We thank Dr. Nagarajan Murali for help with NMR experiments.

Data was obtained at APS beamline 11-ID-B. The authors also thank APS scientists Kevin Beyer, Dr. Olaf Borkiewicz and Dr. Karena Chapman for their assistance with the collection and analysis of this data.

DATA AVAILABILITY

The data that supports the findings of this study are available within the article and its supplementary material.

REFERENCES

- ¹E. W. Castner, Jr. and J. F. Wishart, "Spotlight on Ionic Liquids," J. Chem. Phys. **132**, 120901 (2010).
- ²E. W. Castner, Jr., C. J. Margulis, M. Maroncelli, and J. F. Wishart, "Ionic Liquids: Structure and Photochemical Reactions," Annu. Rev. Phys. Chem. **62**, 85–105 (2011).
- ³K. Ghandi, "A review of ionic liquids, their limits and applications," Green Sustainable Chem. 4, 44–53 (2014).
- ⁴R. Hayes, G. G. Warr, and R. Atkin, "Structure and Nanostructure in Ionic Liquids," Chem. Rev. **115**, 6357–6426 (2015).
- ⁵M. Armand, F. Endres, D. R. MacFarlane, H. Ohno, and B. Scrosati, "Ionic-liquid materials for the electrochemical challenges of the future," Nat. Mater. 8, 621–629 (2009).
- ⁶J. F. Wishart, "Energy applications of ionic liquids." Energy Environ. Sci. **2**, 956–961 (2009).
- ⁷D. R. MacFarlane, N. Tachikawa, M. Forsyth, J. M. Pringle, P. C. Howlett, G. D. Elliott, J. James H. Davis, M. Watanabe, P. Simon, and C. A. Angell, "Energy applications of ionic liquids," Energy Environ. Sci. 7, 232–250 (2014).
- ⁸Z. Zhang, J. Song, and B. Han, "Catalytic transformation of lignocellulose into chemicals and fuel products in ionic liquids," Chem. Rev. **117**, 6834–6880 (2017).
- ⁹M. R. Mosallanejad, M. R. Khosravi-Nikou, and A. Shariati, "Separation of ethanol from n-decane-ethanol mixtures using imidazolium based ionic liquids," J. Chem. Thermodyn. **131**, 471 477 (2019).

- ¹⁰H. Yan, L. Zhao, Y. Bai, F. Li, H. Dong, H. Wang, X. Zhang, and S. Zeng, "Superbase ionic liquid-based deep eutectic solvents for improving CO₂ absorption," ACS Sustain. Chem. Eng. 8, 2523–2530 (2020).
- ¹¹Y. Zhang, X. Ji, Y. Xie, and X. Lu, "Screening of conventional ionic liquids for carbon dioxide capture and separation," Appl. Energy **162**, 1160 1170 (2016).
- ¹²A. Berthod, M. Ruiz-Ángel, and S. Carda-Broch, "Recent advances on ionic liquid uses in separation techniques," J. Chromatogr. A **1559**, 2–16 (2018).
- ¹³E. Boli, E. Dimou, and E. Voutsas, "Separation of the isopropanol-water azeotropic mixture using ionic liquids," Fluid Ph. Equilibria **456**, 77 83 (2018).
- ¹⁴N. Delgado-Mellado, A. Ovejero-Perez, P. Navarro, M. Larriba, M. Ayuso, J. Garca, and F. Rodrguez, "Imidazolium and pyridinium-based ionic liquids for the cyclohexane/cyclohexene separation by liquid-liquid extraction," J. Chem. Thermodyn. 131, 340–346 (2019).
- ¹⁵B. Kabane and G. G. Redhi, "Application of trihexyltetradecylphosphonium dicyanamide ionic liquid for various types of separations problems: Activity coefficients at infinite dilution measurements utilizing glc method," Fluid Ph. Equilibria 493, 181 187 (2019).
- ¹⁶S. M. Urahata and M. C. C. Ribeiro, "Structure of ionic liquids of 1-alkyl-3-methylimidazolium cations: A systematic computer simulation study," J. Chem. Phys. 120, 1855–1863 (2004).
- ¹⁷Y. Wang and G. A. Voth, "Unique Spatial Heterogeneity in Ionic Liquids," J. Am. Chem. Soc. **127**, 12192–12193 (2005).
- ¹⁸A. Triolo, O. Russina, H.-J. Bleif, and E. Di Cola, "Nanoscale segregation in room temperature ionic liquids," J. Phys. Chem. B **111**, 4641–4644 (2007).
- ¹⁹O. Russina, A. Triolo, L. Gontrani, R. Caminiti, D. Xiao, J. Hines, Larry G., R. A. Bartsch, E. L. Quitevis, N. Pleckhova, and K. R. Seddon, "Morphology and intermolecular dynamics of 1-alkyl-3-methylimidazolium bis(trifluoromethane)sulfonylamide ionic liquids: structural and dynamic evidence of nanoscale segregation," J. Phys.: Condens. Matter 21, 424121 (2009).
- ²⁰H. K. Kashyap, C. S. Santos, R. P. Daly, J. J. Hettige, N. S. Murthy, H. Shirota, E. W. Castner, Jr., and C. J. Margulis, "How Does the Ionic Liquid Organizational Landscape Change when Nonpolar Cationic Alkyl Groups Are Replaced by Polar Isoelectronic Diethers?" J. Phys. Chem. B 117, 1130–1135 (2013).

- ²¹K. Shimizu, C. E. S. Bernardes, and J. N. Canongia Lopes, "Structure and Aggregation in the 1-Alkyl-3-Methylimidazolium Bis(trifluoromethylsulfonyl)imide Ionic Liquid Homologous Series," J. Phys. Chem. B **118**, 567–576 (2014).
- ²²B. Wu, H. Shirota, and E. W. Castner, Jr., "Structure of Ionic Liquids with Cationic Silicon-Substitutions," J. Chem. Phys. **145**, 114501 (2016).
- ²³B. Wu, Y. Yamashita, T. Endo, K. Takahashi, and E. W. Castner, Jr., "Structure and Dynamics of Ionic Liquids: Trimethylsilylpropyl-Substituted Cations and Bis(sulfonyl)amide Anions," J. Chem. Phys. 145, 244506 (2016).
- ²⁴M. Zhao, B. Wu, S. I. Lall-Ramnarine, J. D. Ramdihal, K. A. Papacostas, E. D. Fernandez, R. A. Sumner, C. J. Margulis, J. F. Wishart, and E. W. Castner, Jr., "Structural analysis of ionic liquids with symmetric and asymmetric fluorinated anions," J. Chem. Phys. 151, 074504 (2019).
- ²⁵J. N. Canongia Lopes and A. A. H. Padua, "Molecular Force Field for Ionic Liquids III: Imidazolium, Pyridinium, and Phosphonium Cations; Chloride, Bromide, and Dicyanamide Anions," J. Phys. Chem. B 110, 19586–19592 (2006).
- ²⁶J. C. Araque, J. J. Hettige, and C. J. Margulis, "Modern Room Temperature Ionic Liquids, a Simple Guide to Understanding Their Structure and How It May Relate to Dynamics," J. Phys. Chem. B 119, 12727–12740 (2015).
- ²⁷M. Liang, S. Khatun, and E. W. Castner, Jr., "Communication: Unusual Structure and Transport in Ionic Liquid-Hexane Mixtures," J. Chem. Phys. **142**, 121101 (2015).
- ²⁸J. C. Araque, R. P. Daly, and C. J. Margulis, "A Link Between Structure, Diffusion and Rotations of Hydrogen Bonding Tracers in Ionic Liquids," J. Chem. Phys. **144**, 204504 (2016).
- ²⁹W. Schroer, A. Triolo, and O. Russina, "Nature of mesoscopic organization in protic ionic liquidalcohol mixtures," J. Phys. Chem. B **120**, 2638–2643 (2016).
- ³⁰T. Gutel, C. C. Santini, A. A. H. Pádua, B. Fenet, Y. Chauvin, J. N. Canongia Lopes, F. Bayard, M. F. Costa Gomes, and A. S. Pensado, "Interaction between the π-system of toluene and the imidazolium ring of ionic liquids: A combined NMR and molecular simulation study," J. Phys. Chem. B 113, 170–177 (2009).
- ³¹M. Blesic, J. N. C. Lopes, M. F. C. Gomes, and L. P. N. Rebelo, "Solubility of alkanes, alkanols and their fluorinated counterparts in tetraalkylphosphonium ionic liquids," Phys. Chem. Chem. Phys. **12**, 9685–9692 (2010).

- ³²J. N. Canongia Lopes, M. F. Costa Gomes, P. Husson, A. A. H. Pádua, L. P. N. Rebelo, S. Sarraute, and M. Tariq, "Polarity, viscosity, and ionic conductivity of liquid mixtures containing [C4C1im][Ntf2] and a molecular component," J. Phys. Chem. B 115, 6088–6099 (2011).
- ³³M. F. Costa Gomes, L. Pison, A. S. Pensado, and A. A. H. Pádua, "Using ethane and butane as probes to the molecular structure of 1-alkyl-3-methylimidazolium bis[(trifluoromethyl)sulfonyl]imide ionic liquids," Faraday Discuss. **154**, 41–52 (2012).
- ³⁴O. Russina, A. Sferrazza, R. Caminiti, and A. Triolo, "Amphiphile meets amphiphile: Beyond the polarapolar dualism in ionic liquid/alcohol mixtures," J. Phys. Chem. Lett. 5, 1738–1742 (2014).
- ³⁵D. Yalcin, A. J. Christofferson, C. J. Drummond, and T. L. Greaves, "Solvation properties of protic ionic liquidmolecular solvent mixtures," Phys. Chem. Chem. Phys. 22, 10995–11011 (2020).
- ³⁶H. Y. Lee, H. Shirota, and E. W. Castner, Jr., "Differences in Ion Interactions for Isoelectronic Ionic Liquid Homologs," J. Phys. Chem. Lett. 4, 1477–1483 (2013).
- ³⁷L. Gontrani, O. Russina, F. Lo Celso, R. Caminiti, G. Annat, and A. Triolo, "Liquid structure of trihexyltetradecylphosphonium chloride at ambient temperature: An X-ray scattering and simulation study," J. Phys. Chem. B 113, 9235–9240 (2009).
- ³⁸H. K. Kashyap, C. S. Santos, H. V. R. Annapureddy, N. S. Murthy, C. J. Margulis, and E. W. Castner, Jr., "Temperature-Dependent Structure of Ionic Liquids: X-ray Scattering and Simulations," Faraday Discuss. 154, 133–143 (2012).
- ³⁹J. J. Hettige, H. K. Kashyap, and C. J. Margulis, "Communication: Anomalous temperature dependence of the intermediate range order in phosphonium ionic liquids," J. Chem. Phys. 140, 111102 (2014).
- ⁴⁰J. J. Hettige, J. C. Araque, H. K. Kashyap, and C. J. Margulis, "Communication: Nanoscale structure of tetradecyltrihexylphosphonium based ionic liquids," J. Chem. Phys. 144, 121102 (2016).
- ⁴¹Y. Ren, "High-Energy Synchrotron X-Ray Diffraction and Its Application to In-Situ Structural Phase-Transition Studies in Complex Sample Environments," JOM **64**, 140–149 (2012).
- ⁴²E. O. Stejskal, "Use of Spin Echoes in a Pulsed Magnetic Field Gradient to Study Anisotropic, Restricted Diffusion and Flow," J. Chem. Phys. **43**, 3597–3603 (1965).

- ⁴³J. E. Tanner, "Use of the Stimulated Echo in NMR Diffusion Studies," J. Chem. Phys. 52, 2523 (1970).
- ⁴⁴D. Wu, A. Chen, and C. Johnson, "An Improved Diffusion-Ordered Spectroscopy Experiment Incorporating Bipolar-Gradient Pulses," J. Magn. Reson. A115, 260–264 (1995).
- ⁴⁵T. Murphy, R. Hayes, S. Imberti, G. G. Warr, and R. Atkin, "Ionic liquid nanostructure enables alcohol self assembly," Phys. Chem. Chem. Phys. **18**, 12797–12809 (2016).
- ⁴⁶T. Méndez-Morales, J. Carrete, O. Cabeza, O. Russina, A. Triolo, L. J. Gallego, and L. M. Varela, "Solvation of lithium salts in protic ionic liquids: A molecular dynamics study," J. Phys. Chem. B 118, 761–770 (2014).
- ⁴⁷H. Montes-Campos, J. M. Otero-Mato, T. Mndez-Morales, E. Lpez-Lago, O. Russina, O. Cabeza, L. J. Gallego, and L. M. Varela, "Nanostructured solvation in mixtures of protic ionic liquids and long-chained alcohols," J. Chem. Phys. 146, 124503 (2017).
- ⁴⁸I. C. M. Vaz, M. Bastos, C. E. S. Bernardes, J. N. Canongia Lopes, and L. M. N. B. F. Santos, "Solvation of alcohols in ionic liquids—understanding the effect of the anion and cation," Phys. Chem. Chem. Phys. **20**, 2536–2548 (2018).
- ⁴⁹A. Hammersley, S. Svensson, M. Hanfland, A. Fitch, and D. Hausermann, "Two-dimensional detector software: From real detector to idealised image or two-theta scan." High Pressure Res. **14**, 235–248 (1996).
- ⁵⁰X. Qiu, J. W. Thompson, and S. J. L. Billinge, "PDFgetX2: a GUI-driven program to obtain the pair distribution function from X-ray powder diffraction data." J. Appl. Cryst. **37**, 678 (2004).
- ⁵¹H. K. Kashyap, C. S. Santos, N. S. Murthy, J. J. Hettige, K. Kerr, S. Ramati, J. Gwon, M. Gohdo, S. I. Lall-Ramnarine, J. F. Wishart, C. J. Margulis, and E. W. Castner, Jr., "Structure of 1-Alkyl-1-methylpyrrolidinium Bis(trifluoromethylsulfonyl)amide Ionic Liquids with Linear, Branched, and Cyclic Alkyl Groups," J. Phys. Chem. B 117, 15328–15337 (2013).
- ⁵²T. A. Fadeeva, P. Husson, J. A. DeVine, M. F. Costa Gomes, S. G. Greenbaum, and E. W. Castner, Jr., "Interactions Between Water and 1-butyl-1-methylpyrrolidinium Ionic Liquids," J. Chem. Phys. 143, 064503 (2015).
- ⁵³K. B. Dhungana, L. F. O. Faria, B. Wu, M. Liang, M. C. C. Ribeiro, C. J. Margulis, and E. W. Castner, Jr, "Structure of cyano-anion ionic liquids: X-ray scattering and simulations," J. Chem. Phys. 145, 024503 (2016).

- ⁵⁴S. I. Lall-Ramnarine, M. Zhao, C. Rodriguez, R. Fernandez, N. Zmich, E. D. Fernandez, S. B. Dhiman, E. W. Castner, Jr., and J. F. Wishart, "Connecting structural and transport properties of ionic liquids with cationic oligoether chains," J. Electrochem. Soc. 164, H5247–H5262 (2017).
- ⁵⁵B. Wu, K. Kuroda, K. Takahashi, and E. W. Castner, Jr., "Structural analysis of zwitterionic liquids vs. homologous ionic liquids," J. Chem. Phys. 148, 193807 (2018).
- ⁵⁶A. M. Funston, T. A. Fadeeva, J. F. Wishart, and E. W. Castner, Jr., "Fluorescence Probing of Temperature-Dependent Dynamics and Friction in Ionic Liquid Local Environments," J. Phys. Chem. B 111, 4963–4977 (2007).
- ⁵⁷S. H. Chung, R. Lopato, S. G. Greenbaum, H. Shirota, E. W. Castner, Jr., and J. F. Wishart, "A nuclear magnetic resonance study of room temperature ionic liquids with CH₂Si(CH₃)₃ vs. CH₂C(CH₃)₃ substitutions on the imidazolium cations," J. Phys. Chem. B **111**, 4885–4893 (2007).
- ⁵⁸F. Lo Celso, G. B. Appetecchi, E. Simonetti, M. Zhao, E. W. Castner, Jr., U. Keiderling, L. Gontrani, A. Triolo, and O. Russina, "Microscopic Structural and Dynamic Features in Triphilic Room Temperature Ionic Liquids," Front. Chem. 7, 285 (2019).
- ⁵⁹H. V. R. Annapureddy, H. K. Kashyap, P. M. De Biase, and C. J. Margulis, "What is the Origin of the Prepeak in the X-ray Scattering of Imidazolium-Based Room-Temperature Ionic Liquids?" J. Phys. Chem. B 114, 16838–16846 (2010).
- ⁶⁰H. K. Kashyap, J. J. Hettige, H. V. R. Annapureddy, and C. J. Margulis, "SAXS antipeaks reveal the length-scales of dual positive-negative and polar-apolar ordering in room-temperature ionic liquids," Chem. Commun. 48, 5103–5105 (2012).
- ⁶¹R. Serimaa, K. S. Vahvaselk, and M. Torkkeli, "Determination of liquid structures of the primary alcohols methanol, ethanol, 1-propanol, 1-butanol and 1-octanol by x-ray scattering," J. Appl. Crystallogr. 28, 189–195 (1995).
- ⁶²J. Maccallum and D. Tieleman, "Structures of neat and hydrated 1-octanol from computer simulations," J. Am. Chem. Soc. **124**, 15085–93 (2003).
- ⁶³A. Triolo, O. Russina, B. Fazio, G. B. Appetecchi, M. Carewska, and S. Passerini, "Nanoscale organization in piperidinium-based room temperature ionic liquids," J. Chem. Phys. 130, 164521 (2009).
- ⁶⁴R. Elfgen, O. Holloczki, and B. Kirchner, "A molecular level understanding of template effects in ionic liquids," Acc. Chem. Res. **50**, 2949–2957 (2017).

- ⁶⁵E. W. Castner, Jr., J. F. Wishart, and H. Shirota, "Intermolecular Dynamics, Interactions, and Solvation in Ionic Liquids," Acc. Chem. Res. 40, 1217–1227 (2007).
- ⁶⁶H. Jin, B. O'Hare, J. Dong, S. Arzhantsev, G. A. Baker, J. F. Wishart, A. J. Benesi, and M. Maroncelli, "Physical Properties of Ionic Liquids Consisting of the 1-Butyl-3-Methylimidazolium Cation with Various Anions and the Bis(trifluoromethylsulfonyl)imide Anion with Various Cations," J. Phys. Chem. B 112, 81–92 (2008).
- ⁶⁷K. R. Harris, "The fractional Stokes-Einstein equation: Application to Lennard-Jones, molecular, and ionic liquids," J. Chem. Phys. 131, 054503 (2009).
- ⁶⁸J. T. Edward, "Molecular volumes and the stokes-einstein equation," J. Chem. Educ. **47**, 261 (1970).
- ⁶⁹S. Agrawal and H. K. Kashyap, "Structures of binary mixtures of ionic liquid 1-butyl-3-methylimidazolium bis(trifluoromethylsulfonyl)imide with primary alcohols: The role of hydrogen-bonding," J. Mol. Liq., (2018).
- ⁷⁰T. Iwahashi, Y. Sakai, K. Kanai, D. Kim, and Y. Ouchi, "Alkyl-chain dividing layer at an alcohol/ionic liquid buried interface studied by sum-frequency generation vibrational spectroscopy," Phys. Chem. Chem. Phys. 12, 12943–12946 (2010).
- ⁷¹T. Iwahashi, Y. Sakai, D. Kim, T. Ishiyama, A. Morita, and Y. Ouchi, "Nonlinear vibrational spectroscopic studies on water/ionic liquid([C(n)mim]TFSA: n=4, 8) interfaces," Faraday Discuss. **154**, 289–301 (2012).